OXFORD

Human Molecular Genetics, 2022, Vol. 31, No. 5 705–717

https://doi.org/10.1093/hmg/ddab284
Advance Access Publication Date: 27 September 2021
General Article

GENERAL ARTICLE

α-synuclein inhibits Snx3-retromer retrograde trafficking of the conserved membrane-bound proprotein convertase Kex2 in the secretory pathway of *Saccharomyces cerevisiae*

Santhanasabapathy Rajasekaran[1,†], Patricia P. Peterson[2], Zhengchang Liu[2], Lucy C. Robinson[1] and Stephan N. Witt[1,*,‡]

[1]Department of Biochemistry and Molecular Biology, Louisiana State University Health Sciences Center, Shreveport, LA 71103 USA and [2]Department of Biological Sciences, The University of New Orleans, New Orleans, LA 70148 USA

*To whom correspondence should be addressed at: 1501 Kings Highway, Shreveport, LA 71103, USA. Tel: +1 3186755163; Fax: +1 3186755180; E-mail: stephan.witt@lsuhs.edu

Abstract

We tested the ability of alpha-synuclein (α-syn) to inhibit Snx3-retromer-mediated retrograde trafficking of Kex2 and Ste13 between late endosomes and the *trans*-Golgi network (TGN) using a *Saccharomyces cerevisiae* model of Parkinson's disease. Kex2 and Ste13 are a conserved, membrane-bound proprotein convertase and dipeptidyl aminopeptidase, respectively, that process pro-α-factor and pro-killer toxin. Each of these proteins contains a cytosolic tail that binds to sorting nexin Snx3. Using a combination of techniques, including fluorescence microscopy, western blotting and a yeast mating assay, we found that α-syn disrupts Snx3-retromer trafficking of Kex2-GFP and GFP-Ste13 from the late endosome to the TGN, resulting in these two proteins transiting to the vacuole by default. Using three α-syn variants (A53T, A30P, and α-synΔC, which lacks residues 101–140), we further found that A53T and α-synΔC, but not A30P, reduce Snx3-retromer trafficking of Kex2-GFP, which is likely to be due to weaker binding of A30P to membranes. Degradation of Kex2 and Ste13 in the vacuole should result in the secretion of unprocessed, inactive forms of α-factor, which will reduce mating efficiency between *MAT*a and *MAT*α cells. We found that wild-type α-syn but not A30P significantly inhibited the secretion of α-factor. Collectively, our results support a model in which the membrane-binding ability of α-syn is necessary to disrupt Snx3-retromer retrograde recycling of these two conserved endopeptidases.

Introduction

Parkinson's disease (PD) is the second most common neurodegenerative disease and the most common movement disorder, and the main risk factor is age (1). The disease is due to the progressive degeneration of the dopaminergic neurons in the mid-brain, and the loss of dopamine leads to a constellation of motor and non-motor symptoms. Inclusion bodies, called Lewy bodies, form in the affected neurons, and their principal component are the presynaptic protein alpha-synuclein (α-syn)

†Santhanasabapathy Rajasekaran, http://orcid.org/0000-0002-3531-2448
‡Stephan N. Witt, http://orcid.org/0000-0002-6462-2840
Received: July 1, 2021. **Revised:** September 20, 2021. **Accepted:** September 21, 2021

(2,3). α-syn has been implicated in sporadic PD (3), and missense mutations (4–8) or multiplications of the α-syn gene (9) cause early-onset PD (10). Although the exact function of α-syn is not known, the protein appears to regulate endocytosis and exocytosis (11–14). Composed of only 140 amino acids, α-syn is a structural chameleon: it is an unstructured monomer in solution (15), an α-helical monomer when bound to membranes (16), a soluble four helix bundle of monomers (17), soluble oligomeric structures (18) and insoluble β-sheet amyloid fibers (19). Soluble oligomeric species of α-syn likely kill cells by permeabilizing organelles and vesicles (20,21).

Genetic studies of PD patients have implicated a defect in endocytosis as a cause of some cases of early-onset PD. Specifically, mutations in the conserved gene *VPS35*, which encodes a component of the endocytic recycling complex called retromer, occur in some patients with early-onset PD (22–24). Retromer is a multimeric protein complex that sorts, exports, and retrieves membrane-bound cargo proteins embedded in early endosomes (25–27). Retromer is composed of two sub-complexes that coat the cytosolic face of early endosomes (Fig. 1). The Vps26-Vps29-Vps35 (hVps26, hVps29, hVps35 in humans) (28) trimer binds cargo proteins, whereas the membrane-associated Vps5-Vps17 (Snx1 and Snx2 in humans) heterodimer deforms endosomes into tubules (37,38). Vps5 and Vps17 are sorting nexins, each of which contains a phox homology domain that selectively binds to phosphatidylinositol 3′-phosphate (PI3P) (29) and a BIN/Amphiphysin/Rvs domain that senses membrane curvature and remodels endosomes into tubules (30). Upon endocytosis of a cell surface receptor, to prevent the endosomes and receptors from trafficking to the lysosome for degradation, the retromer complex must bind to the sorting signal of the receptor that sticks out into the cytoplasm, and this is followed by the formation of endosomal tubules from which retromer-cargo vesicles bud off and then transit to the *trans*-Golgi network (TGN) for recycling to the plasma membrane (31). Adding complexity, some vesicular trafficking pathways in cells use Snx3-retromer complexes, and Snx3 binds to cargo proteins that have a specific C-terminal endocytic recycling sequence (31).

In *Saccharomyces cerevisiae*, Snx3-retromer mediates the retrograde recycling of cell-surface proteins in the early-endosome-to-TGN and late-endosome-to-TGN pathways. For example, Snx3-retromer mediates the retrograde recycling of the high-affinity iron import pair of proteins Fet3 and Ftr1 from the plasma membrane in early endosomes to the TGN under low iron conditions (Fig. 1A), and when iron levels increase, endocytosed Fet3-Ftr1 molecules are shunted to the vacuole for degradation (32–37). Snx3-retromer also functions in the secretory pathway. Kex1, Kex2 and Ste13 are conserved membrane-bound proprotein convertases that process pro-α-factor and pro-killer toxin for secretion (38). Each of these proteins has a Golgi retention signal in their cytoplasmic tails (39,40). These resident TGN proteins also transit into late endosomes, and Snx3-retromer retrieves them back to the TGN (39,41–43). If *SNX3* is deleted, Kex2 molecules shunt to the vacuole by default (32,44). The cytoplasmic tails of these three enzymes contain an endocytic recycling sequence that binds to Snx3 (36,44).

We have previously shown that α-syn disrupts Snx3-retromer retrograde recycling of Fet3-Ftr1 (Fig. 1B) by interfering with the binding of Snx3 and Vps17 to endosomes in *S. cerevisiae* (45). We proposed that α-syn inhibits the binding of Snx3 and Vps17 to the anionic phospholipid PI3P on the cytoplasmic face of endosomes. When Snx3 and Vps17 fail to bind to endosomes containing Fet3-Ftr1 complexes, the complexes are shunted to the vacuole by default. To test the generalizability of our model, we asked whether α-syn can disrupt the recycling of the two Snx3 cargo proteins, Kex2 and Ste13 (Fig. 1B). Kex2 is an ideal protein to study because it is a highly conserved Ca^{2+}-dependent subtilisin/kexin proprotein convertase, also called a proprotein convertase, which has numerous human orthologs, some of which are expressed in neurons.

We show that α-syn, A53T, and α-synΔC, but not A30P, partially blocks the Snx3-retromer-mediated recycling of Kex2 between the TGN and pre-vacuolar endosomal compartments, which results in its transiting to the vacuole. A similar effect of α-syn on Snx3-retromer trafficking of Ste13 is also found. Strikingly, α-syn, but not A30P, also inhibits the Ste13- and Kex2-dependent mating response.

Results

It is useful to know that in mammalian cells the Golgi apparatus is perinuclear, whereas in *S. cerevisiae*, the Golgi apparatus is scattered throughout the cell, and that the yeast late-Golgi compartment is thought to be functionally equivalent to the mammalian TGN (32). The term TGN is used herein. Snx3, which was originally named Grd19, was identified in a genetic screen that identified genes that when mutated failed to retain Kex2 in the TGN (46). This unique group of genes was named **G**olgi **r**etention **d**eficient.

Ste13, which is a conserved integral membrane dipeptidyl aminopeptidase that processes α-factor (47), is a resident TGN protein (Fig. 2). Ste13 has human orthologs. Although it is a resident TGN protein, Ste13 also partially distributes to endosomal compartments (but not the plasma membrane). The effect of α-syn on the localization of a green fluorescent protein-Ste13 fusion (GFP-Ste13) was evaluated in the budding yeast *S. cerevisiae*. A BY4742 *ste13*Δ mutant was sequentially transformed with two plasmids: one plasmid harbored *GFP-STE13*, and the other plasmid harbored the human α-syn insert under the control of the *GAL1* promoter or empty vector. Figure 3A shows fluorescence microscopic images of cytoplasmic puncta of Ste13-GFP (row 1), which we interpret to be Golgi and/or endosomal vesicles (43). The number of these puncta per cell decreased upon expression of α-syn (row 2). When similar experiments were performed in the *ste13*Δ *snx3*Δ strain (rows 3 and 4), very few puncta were visible in this strain; instead, green fluorescence appeared in the vacuoles. Quantitative analysis of the fluorescence images obtained from three independent clones shows that α-syn decreased the percentage of cells exhibiting green Golgi/endosome puncta by 23% ($P < 0.0001$), whereas *snx3*Δ abolished nearly all puncta (Fig. 3B). Figure 3C shows that α-syn was expressed in the strains of interest.

We also determined whether α-syn disrupts Snx3-retromer-mediated trafficking of the integral membrane, Ca^{2+}-dependent proprotein convertase Kex2, which is a member of the subtilisin/kexin family of serine endoproteases that is found in prokaryotic and eukaryotic organisms (48) (Fig. 2). Kex2 has several human orthologs, including human proprotein convertase PCSK1 (Supplementary Material, Fig. S1).

We first sought to verify that *snx3*Δ abolished the Golgi-endosomal puncta of Kex2-GFP, as reported by Voos and Stevens (44). Two BY4742 strains were used: the parent strain, which had a chromosomally integrated copy of *KEX2-GFP* replacing the wild-type allele, and an isogenic *snx3*Δ mutant. Figure 4A shows fluorescence microscopic images of cytoplasmic puncta of Kex2-GFP (row 1), which we interpret to be Golgi and/or late endosomal vesicles (49). Similar experiments were performed in the

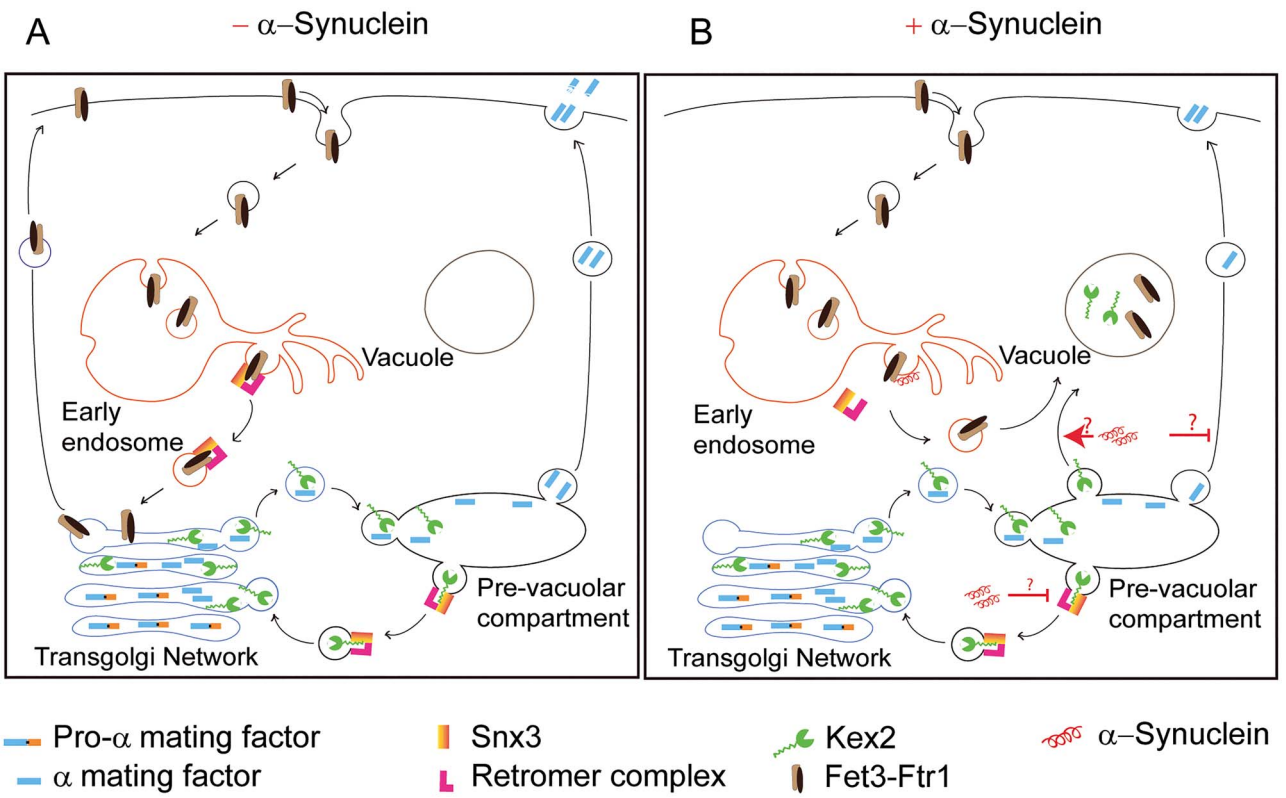

Figure 1. Snx3-retromer functions in yeast. (**A**) Snx3-retromer mediates the retrograde trafficking of Fet3-Ftr1 from the plasma membrane to the TGN under conditions of iron starvation. These two proteins function to import iron into the cell. An increase in ambient iron results in the default pathway: endocytosed Fet3-Ftr1 molecules shunt to the vacuole for degradation. Snx3-retromer also retrieves Kex2 and Ste13 from the pre-vacuolar compartment/late endosome to the TGN. (**B**) The expression of α-syn in yeast cells under iron-starved conditions results in Fet3-Ftr1 molecules following the default pathway to the vacuole. It is proposed that α-syn also disrupts the Snx3-retomer-dependent retrieval of Kex2 from late endosomes, resulting in Kex2 transiting to the vacuole by default. Snx3-retromer also retrieves Ste13 from late endosomes, but this is not shown for simplicity.

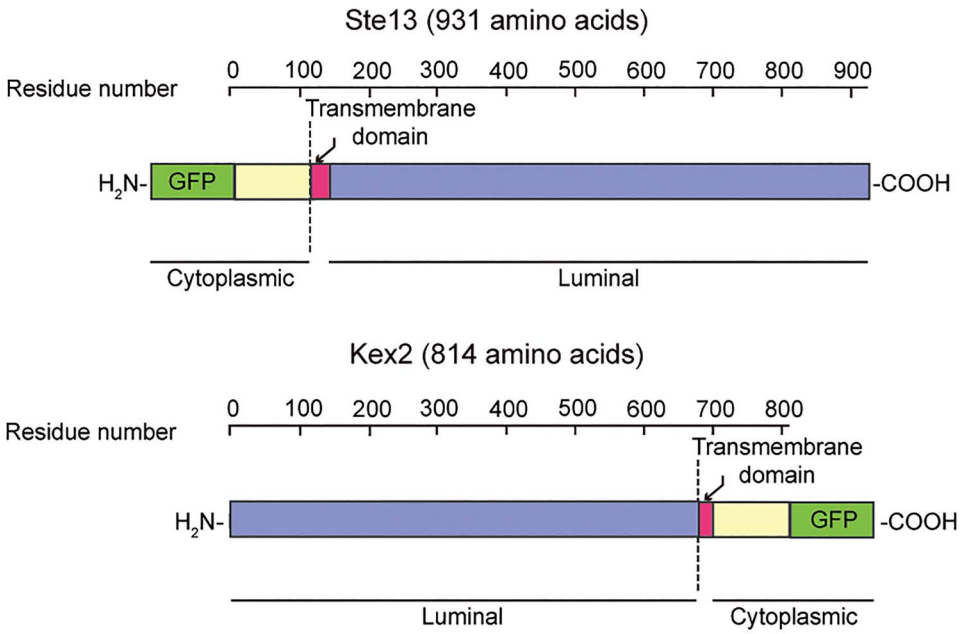

Figure 2. The domain structure of Kex2 and Ste13. These proteins are synthesized as pro-proteins and undergo processing, which includes proteolytic removal of certain domains as well as glycosylation, to achieve the active state. For details on the processing of Kex2 see ref (65).

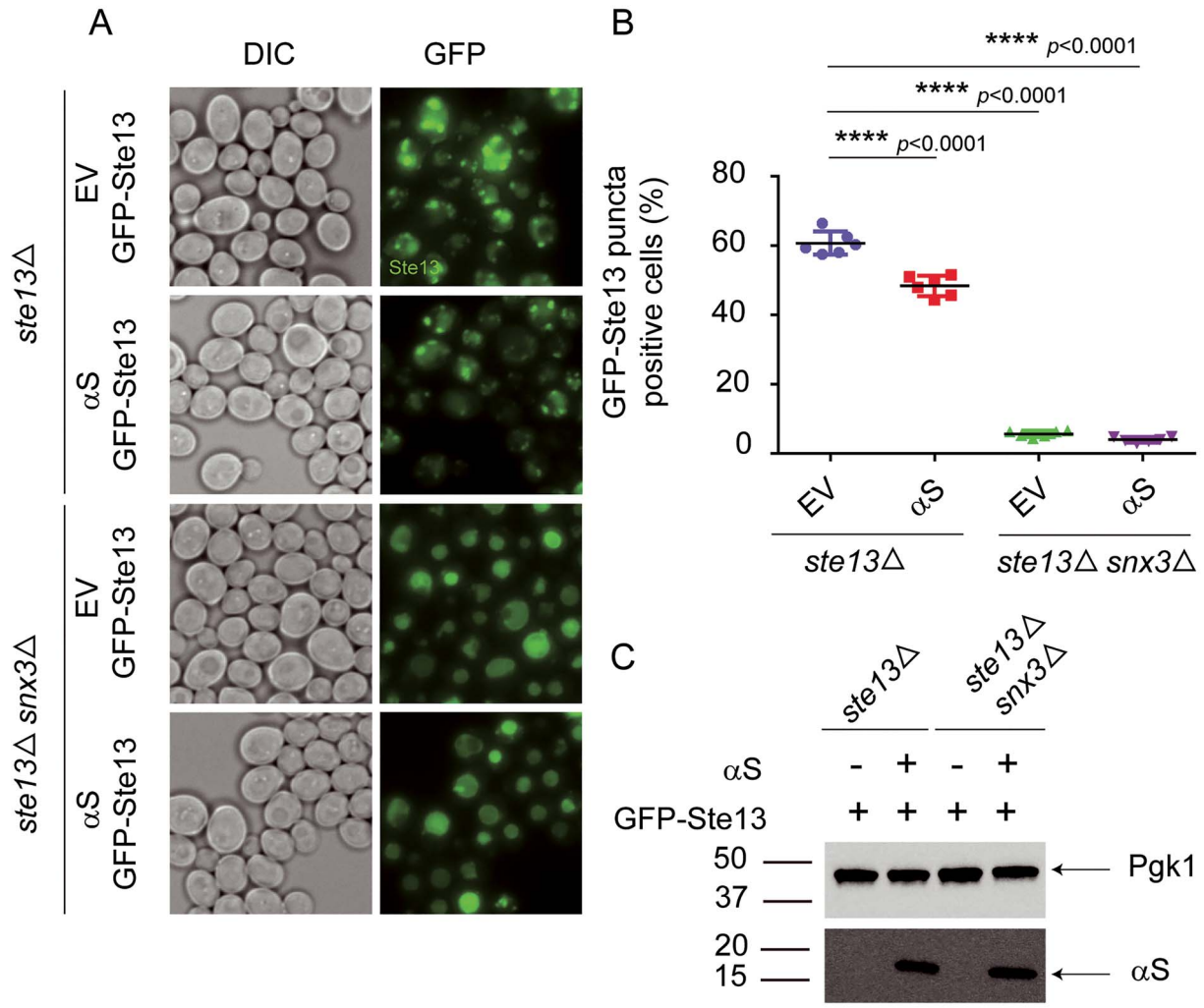

Figure 3. Sorting nexin Snx3 is required for the formation of cytoplasmic foci of Ste13-GFP. (**A**) Microscopic analysis of cellular localization of GFP-Ste13 in *ste13Δ* cells carrying a plasmid encoding *GFP-STE13* and a plasmid encoding α-syn or the empty vector as control. (**B**) Plot of the percentage of Ste13-GFP puncta-positive cells in the indicated strains. Three clones were evaluated; cells were counted in two random fields (300 cells) per clone; one-way ANOVA with Bonferroni correction was used in statistical analysis. (**C**) Western blot analysis of α-syn expression in the strains as indicated. Pgk1 is included as loading controls.

KEX2-GFP snx3Δ strain (row 2). Very few puncta were visible in the mutant strain; instead, diffuse green fluorescence appeared in the vacuoles. Figure 4B shows that the cellular localization of Kex2-GFP was unaffected by the introduction of an empty vector. We also demonstrated that re-expressing Snx3 (in the form Snx3-mCherry) in the *KEX2-GFP snx3Δ* strain quantitatively restored Kex2-GFP cellular localization to green puncta attributable to Golgi/endosomal vesicles (Fig. 4C and D). Western blotting of cell lysates showed that Kex2-GFP was detectable in the *KEX2-GFP snx3Δ* strain carrying a plasmid encoding *SNX3-mCherry*, whereas the level of Kex2-GFP was reduced by ∼60% in cells harboring the empty vector (Fig. 4E and F). The results show that Golgi/endosomal localization of Kex2-GFP is largely abolished when the sorting nexin Snx3 is absent from cells, and that in this case Kex2-GFP is targeted to the vacuoles for degradation.

We then determined whether α-syn affects the trafficking of Kex2-GFP. Figure 5A shows fluorescence microscopic images of cytoplasmic puncta of Kex2-GFP (row 1). Quantitative analysis of multiple clones revealed that 80% of *GFP-KEX2*-expressing cells carrying an empty vector displayed cytoplasmic puncta and expressing α-syn in these cells significantly decreased the percentage of cells exhibiting such puncta to 55% ($P < 0.0001$) (Fig. 5A and B). Similar experiments were performed in the *KEX2-GFP snx3Δ* strain (Fig. 5A, rows 3 and 4) and we found that <10% of cells exhibited cytoplasmic puncta in both the presence or absence of a plasmid encoding α-syn. Instead, green fluorescence appeared in the vacuoles in most *snx3Δ* mutant cells (Fig. 5, A and B). To augment the fluorescence microscopy experiments, the level of Kex2-GFP in both wild-type and *snx3Δ* mutant strains with and without α-syn expression was monitored (Fig. 5C and D). Expression of α-syn in otherwise wild-type cells or *snx3Δ* resulted in significant decreases in the level of the Kex2-GFP protein, consistent with its degradation in the vacuole (Fig. 5D). The combined results in Figures 3–5 show that that α-syn disrupts the Snx3-retromer trafficking of Ste13 and Kex2, but never to the same extent as deleting *SNX3*.

Seven missense mutations in the gene that codes for α-syn (*SNCA*) have been identified, and individuals who have one of these mutations suffer from autosomal dominant, early-onset PD (1). These missense mutations yield α-syn variants A30P, A53T, E46K, H50Q, G51D, A53E, and A53V (4–8,50,51). C-terminal

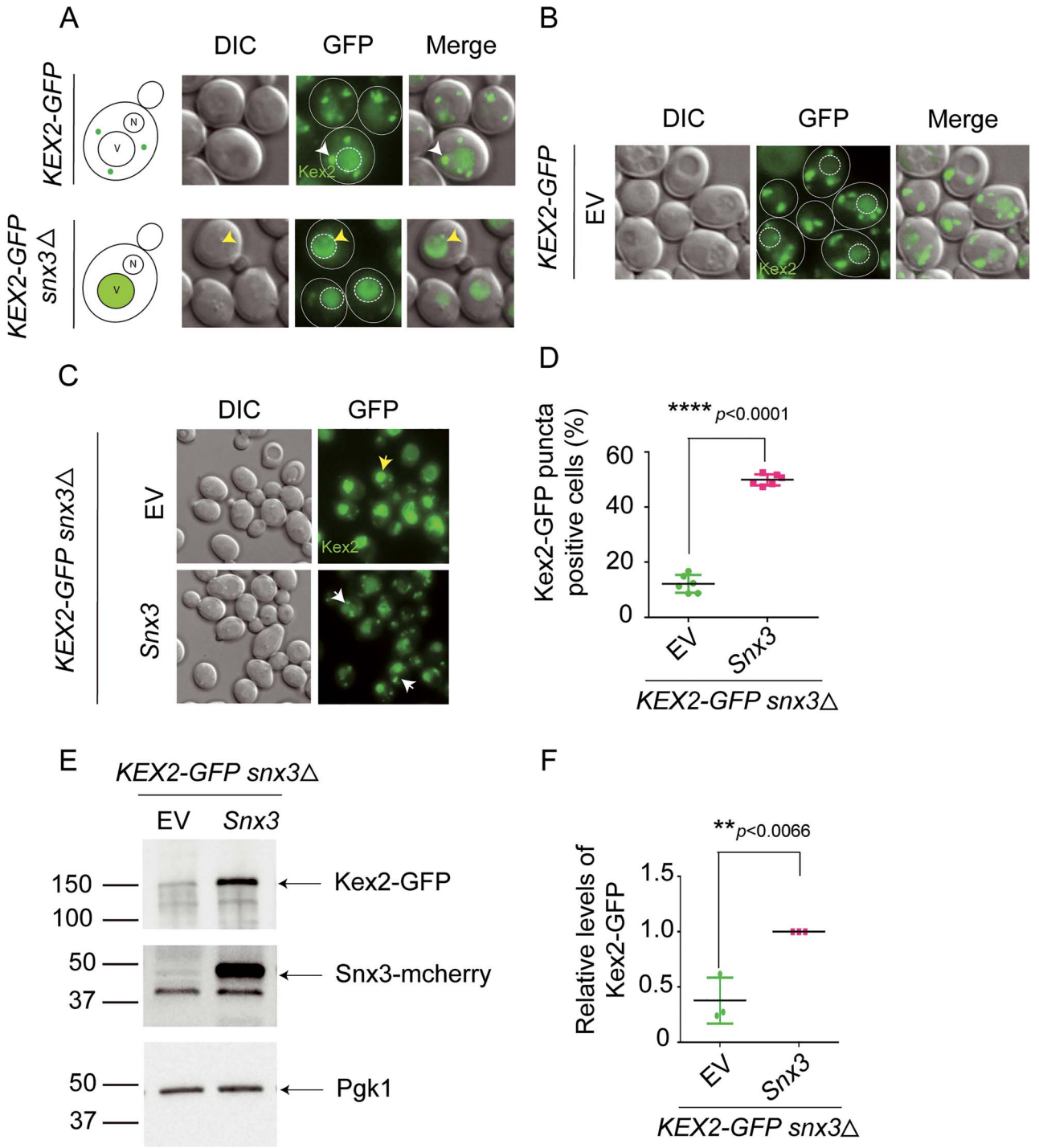

Figure 4. Fluorescence microscopy shows that sorting nexin Snx3 is required for the formation of cytoplasmic foci of Kex2-GFP. (**A**) Fluorescence microscopic analysis of cellular localization of Kex2-GFP in wild-type and *snx3Δ* mutant cells. In the *KEX2-GFP* strain, Kex2-GFP predominantly localizes to cytoplasmic foci (white arrowhead). In the *KEX2-GFP snx3Δ* strain, cells are largely devoid of Kex2-GFP cytoplasmic foci; instead, Kex2-GFP localizes to the vacuoles (yellow arrowhead). For clarity, in the GFP images cell perimeters are denoted by a continuous white line and vacuoles are denoted by a dashed white line. (**B**) Cellular localization of Kex2-GFP in the *KEX2-GFP* strain carrying the empty vector (EV, pAG426Gal). White lines denote perimeters of the cells and vacuoles. (**C**) Re-expressing Snx3 (as Snx3-mCherry) in the *KEX2-GFP snx3Δ* strain restores the localization of Kex2-GFP to cytoplasmic foci. Yellow arrow denotes Kex2-GFP in the vacuole; white arrows denote cytoplasmic foci of Kex2-GFP. (**D**) Plot of the percentage of Kex2-GFP puncta-positive cells in the indicated strains. Three clones were evaluated; cells were counted in two random fields (300 cells) per clone; Student's *t*-test was used in statistical analysis. (**E**) Western blot analysis of the expression of Kex2-GFP and Snx3-mCherry. Cellular lysates were subjected to SDS-PAGE followed by western blotting to detect Kex2-GFP (with anti-GFP antibody), Snx3-mCherry (with anti-mCherry antibody) and the loading control Pgk1. The band at ~40 kDa in both lanes is a non-specific band. (**F**) Quantification of Kex2-GFP levels in the indicated strains from western blot data. Student's t-test was used in statistical analysis (N = 3). Microscopy (A–D) and western blotting (E, F) were conducted with a 5 h and 10 h induction in galactose, respectively.

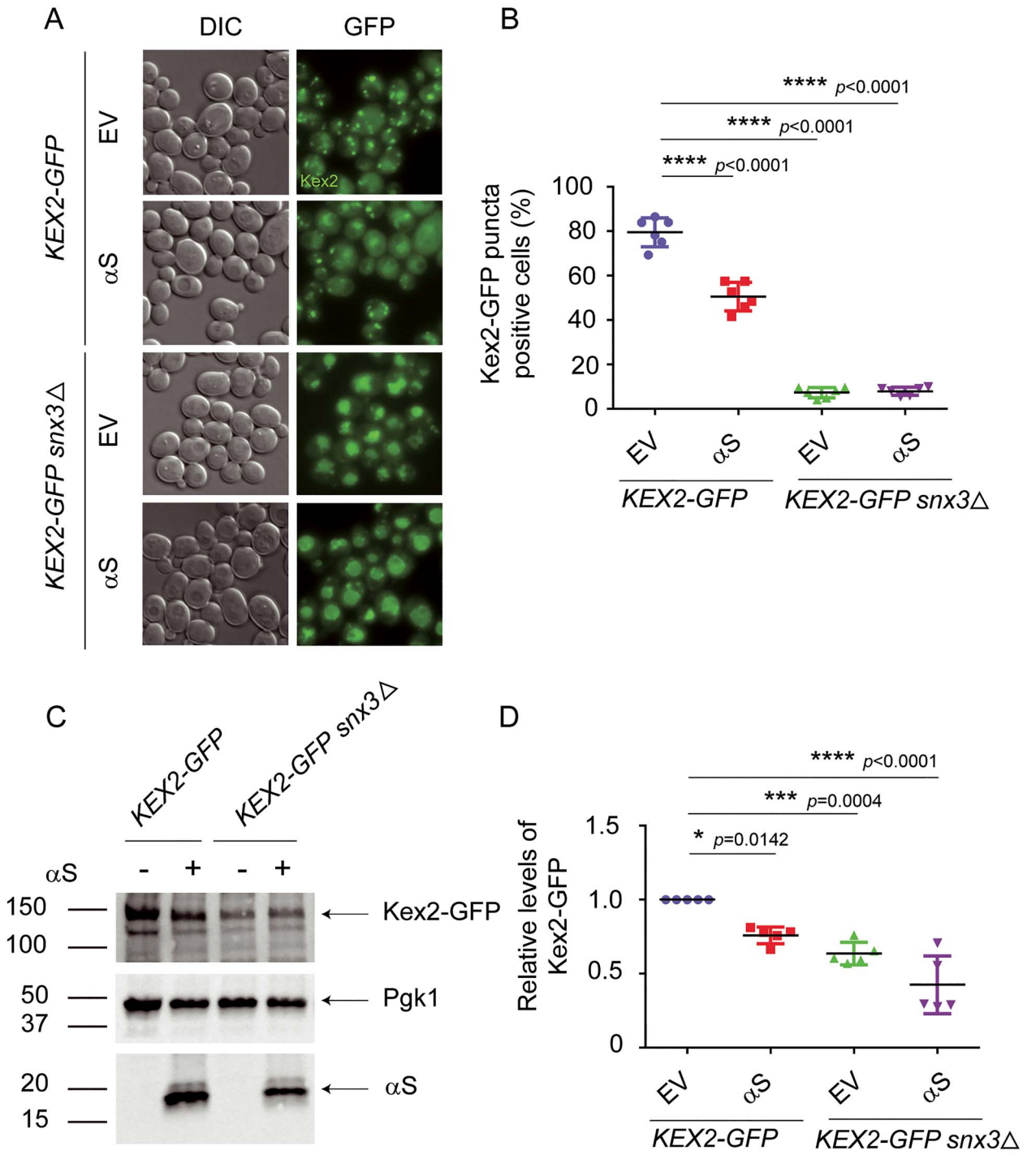

Figure 5. α-syn decreases the number of cells with cytoplasmic foci of Kex2-GFP but not as efficiently as *snx3Δ*. (**A**) α-syn decreases the number of cells exhibiting Kex2-GFP cytoplasmic foci, whereas *snx3Δ* almost completely eliminates these foci. (**B**) Quantitative analysis of the percentage of cells with puncta localization of Kex2-GFP in the indicated strains. Three clones were evaluated; cells were counted in two random fields (300 cells) per clone; one-way ANOVA with Bonferroni correction was used in statistical analysis. (**C**) Western blot analysis of Kex2-GFP and α-syn. Cellular lysates were subjected to SDS-PAGE followed by western blotting to detect Kex2-GFP (with anti-GFP antibody), α-syn, and the loading control Pgk1. (**D**) Quantitative analysis of Kex2-GFP expression shows that the expression of α-syn significantly decreases the level of Kex2-GFP. One-way ANOVA with Bonferroni correction was used in statistical analysis (N = 5).

truncated variants of α-syn have also been reported to rapidly aggregate and are found in Lewy bodies (52,53). In the following experiments, we assessed whether A30P, A53T and α-synΔC (lacking residues 101–140) were as effective as wild-type α-syn in disrupting the trafficking of Kex2. The A30P variant is of particular interest because it fails to bind to membranes to the

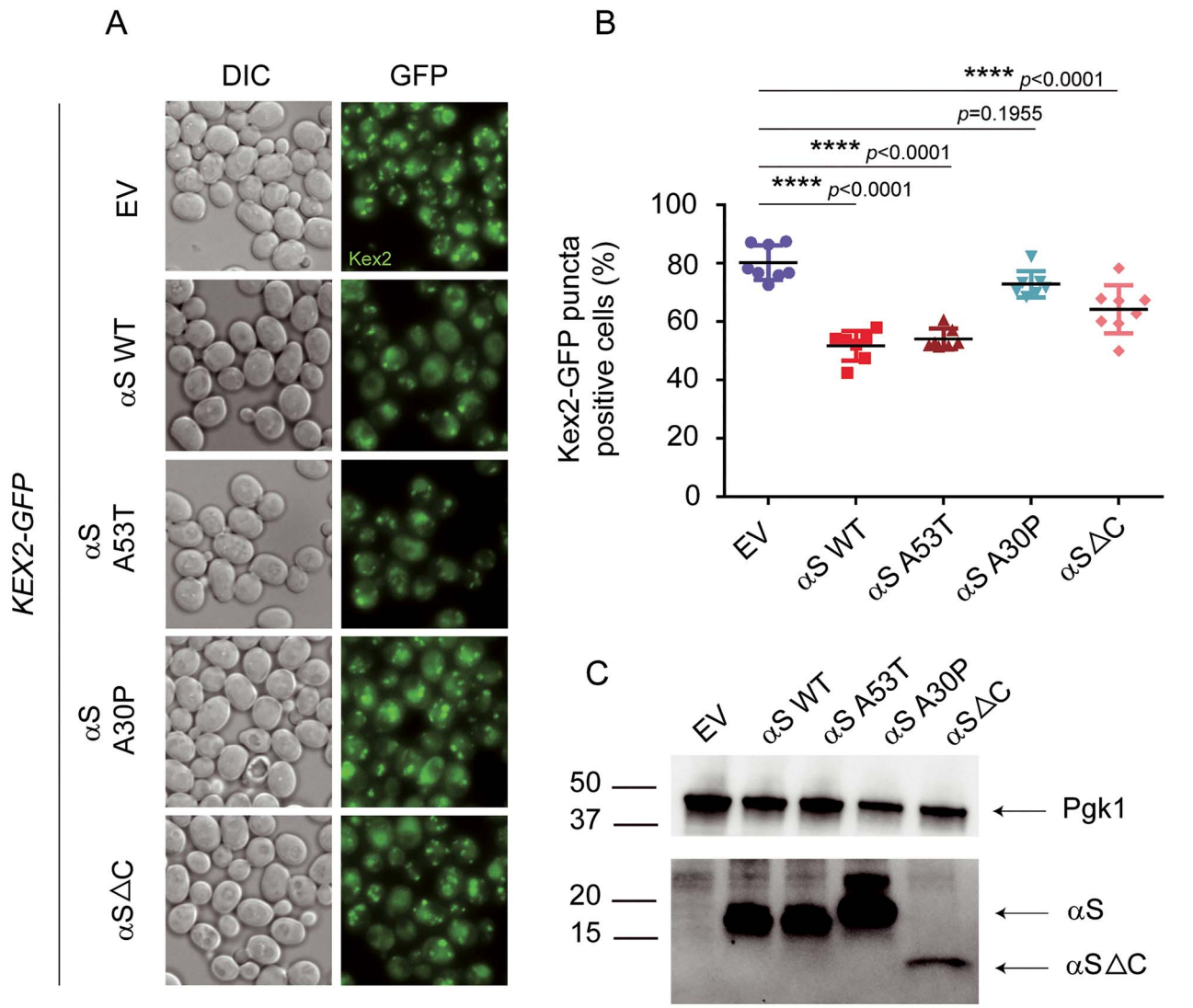

Figure 6. The effects of α-syn and its mutants (A30P, A53T and α-synΔC) on the cellular localization of Kex2-GFP. (**A**) Microscopic analysis of cellular localization of Kex2-GFP. *KEX2-GFP* cells carrying the indicated plasmids were induced for 5 h in galactose to analyze the effect of synucleins on Kex2-GFP localization. (**B**) Quantitative analysis of the percentage of cells showing puncta localization of Kex2-GFP in *KEX2-GFP* cells carrying the indicated plasmids. Four clones were evaluated; cells were counted in two random fields (300 cells) per clone; one-way ANOVA with Dunnett post hoc test was used in statistical analysis. (**C**) Western blot analysis of the expression of α-syn and its variants.

same extent as wild-type α-syn or A53T (54,55). According to our proposed model (45), A30P should fail to disrupt or partially disrupt Snx3-retromer-mediated trafficking of Kex2, and this was tested as follows.

The effects of three α-syn variants on the localization of Kex2-GFP were assessed by fluorescence microscopy (Fig. 6A). Distinct green cytoplasmic puncta were seen in the empty vector control strain (Fig. 6A, row 1). A decrease in the number of these green puncta occurred in cells expressing α-syn, A53T and α-synΔC (Fig. 6A, rows 2, 3 and 5), whereas cells expressing A30P did not appear to affect the cellular localization of Kex2-GFP (Fig. 6A, row 4). Hundreds of cells from multiple clones for each condition were counted to determine the percentage of cells exhibiting the Golgi/endosomal puncta (Fig. 6B). Statistically significant decreases in the percentage of cells exhibiting Golgi/endosomal puncta from Kex2-GFP were found for wild-type α-syn, A53T and α-synΔC, but not for A30P, compared with control cells. Figure 6C shows the expression of the various α-syn proteins.

Given that Ste13 and Kex2 endoproteases are essential for the processing and secretion of α-factor and that wild-type α-syn, but not the A30P variant, disrupts the trafficking of both endoproteases, we hypothesized that α-syn but not A30P should inhibit the maturation of α-factor and thus mating. Secreted α-factor can be detected in a simple plate assay of growth inhibition of super-sensitive *MAT*a cells lacking the Bar1 protease ('barrier factor') as a halo around the α-factor source. This assay can be used quantitatively, as the size of the halo of growth inhibition is related mathematically to the concentration of α-factor to which the lawn of *bar1*Δ strain is exposed (56). The assay is effective no matter whether the lawn of sensitive cells is exposed to a point source of pure α-factor or to cells expressing α-factor. Thus, the ability of cells to secrete mature α-factor can be assessed by the halo assay, comparing the sizes of halos

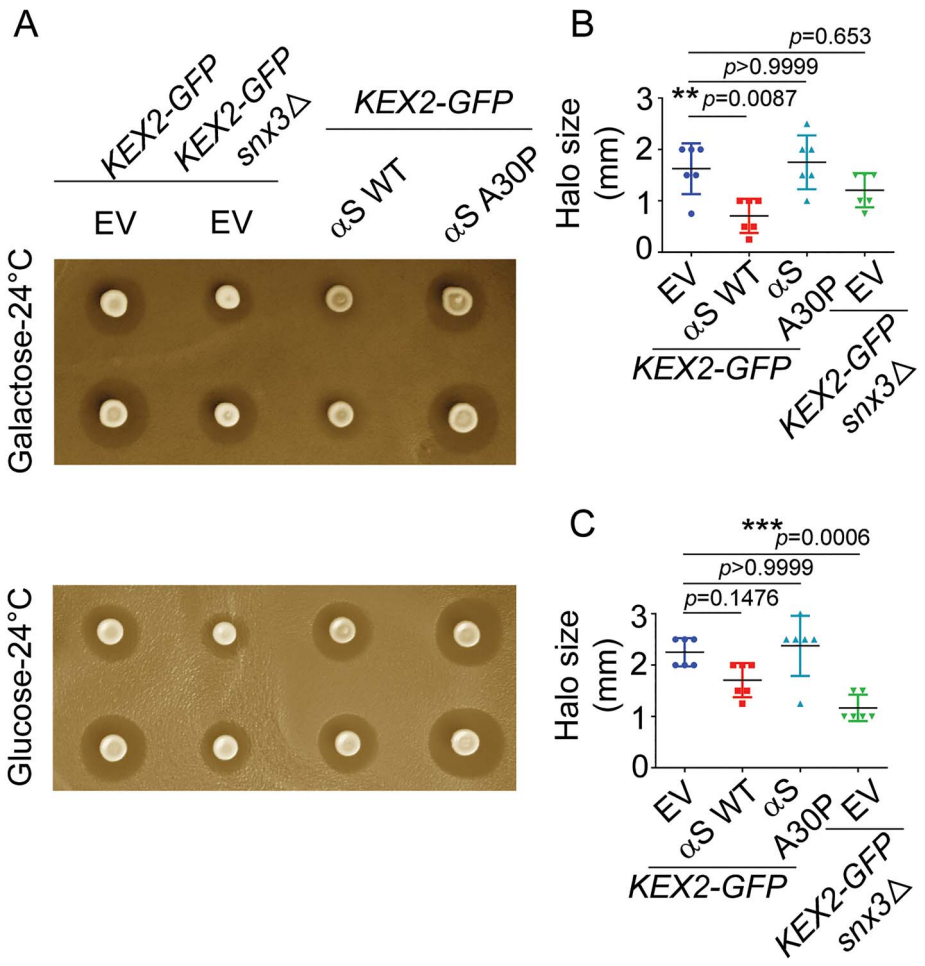

Figure 7. Halo size reduction indicates decreased secretion and/or maturation of the α-factor upon expression of α-syn. (**A**) Growth inhibition of a lawn of reporter strain KT1381, lacking the Bar1 protease, results in halos surrounding α-factor-producing cells. Test strains were grown in non-inducing medium and shifted to inducing medium for 4 h before plating on the lawn of reporter cells as described in Materials and Methods. Tests were carried out in duplicate on each plate shown. (**B** and **C**) Quantitation of halo sizes from plates. Data from six experimental replicates were analyzed as described in Materials and Methods.

produced in response to wild-type cells to those produced in response to cells deficient in some aspect of α-factor production, processing or secretion. To assess whether yeast *MAT*α cells expressing α-syn or A30P produce and secrete α-factor normally, we carried out halo assays, plating a constant number of cells on a lawn of sensitive cells and measuring the zone of growth inhibition.

For the *KEX2-GFP* strains transformed with the empty vector, α-syn or A30P plasmid, under inducing conditions, the halos caused by cells carrying the empty vector or the A30P plasmid were of nearly identical size, whereas the cells expressing α-syn exhibited a significant ($P = 0.0087$) reduction in halo size relative to the control EV cells (Fig. 7A, top panel and B). For the *KEX2-GFP snx3*Δ strain carrying the empty vector under inducing conditions, the size of halos was reduced, which was not statistically significant when compared with the *KEX2-GFP* strain carrying the empty vector. The same experiments were conducted under non-inducing conditions (glucose), and in this case, as expected because of the lack of expression, the reduction in halo size by α-syn was not significant (Fig. 7A, bottom panel and C). Together, the mating assay results indicate that wild-type α-syn, but not the A30P variant, inhibits the secretion or maturation of the α-factor.

Discussion

In this study, we showed that wild-type α-syn, A53T, and α-synΔC, but not A30P, disrupt Snx3-retromer-mediated trafficking of Kex2 (and possibly Ste13 as well) between the pre-vacuolar/late endosomal compartment and TGN, and, strikingly, a biologic consequence is a reduction in the secretion or maturation of α-factor (Fig. 8). Overall, these results are consistent with our model in which α-syn inhibits the binding of Snx3 (and retromer component Vps17) to endosomes, resulting in cargo mis-localizing to the vacuole (Fig. 8).

α-syn localizes to presynaptic membranes in dopaminergic neurons, where it coats synaptic vesicles docked at the presynaptic membranes (13). Missense mutations of α-syn cluster in its N-terminal region, which is the region that forms an α-helix when the protein binds to membranes. In A30P α-syn, the proline at position 30 likely prevents the protein from adopting an α-helical conformation that is required for membrane binding; consequently, A30P binds much less, if at all, to membranes and vesicles. We found that A30P failed to affect Snx3-retromer trafficking of Kex2-GFP, as judged by the formation of Golgi and endosomal punctate structures like those that formed in control cells (Fig. 6). Strikingly, A30P caused no significant reduction in

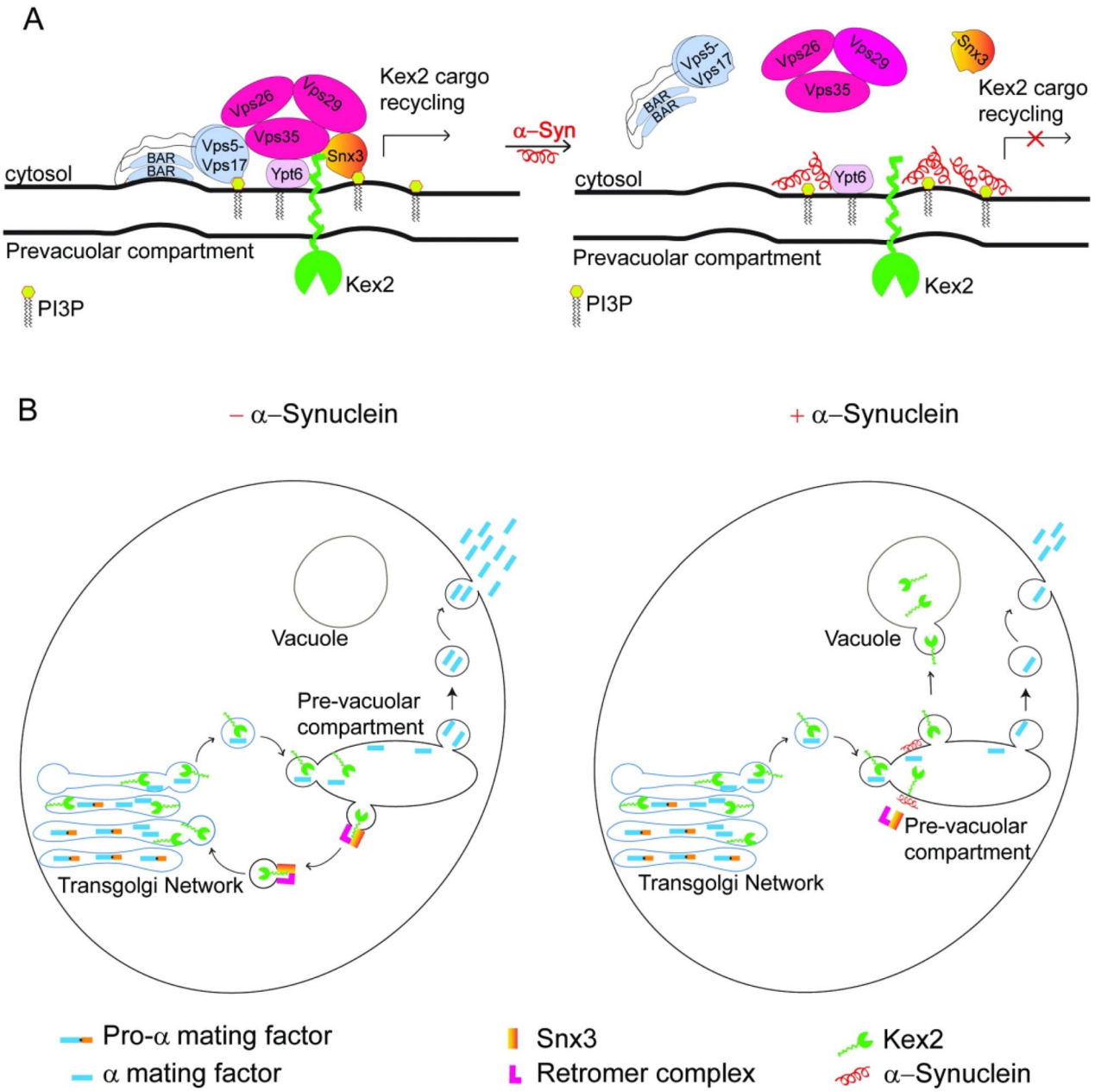

Figure 8. A model on the inhibition of Snx3-retromer-mediated retrieval of Kex2 from the pre-vacuolar compartment to TGN by α-syn. (**A**) α-syn binds to PI3P, and this binding inhibits the binding of Snx3-retromer to the endosome surface. The cargo, Kex2, then trafficks by default to the vacuole. (**B**) In the absence of α-syn, Kex2 (and Ste13) cycle between the pre-vacuolar compartment and the trans-Golgi in a Snx3-retromer dependent manner. α-syn disrupts Snx3-retromer association with PI3P, resulting in the mis-processing of α-factor and concomitant degradation of Kex2 in the vacuole.

the activity of the α-factor (Fig. 7). A30P, which has very low affinity for membranes, would be expected to have little to no effect on Snx3-retromer-mediated trafficking of cargo, possibly because it cannot inhibit the binding of Snx3 to PI3P. These results strongly support our model for how α-syn inhibits Snx3-retromer trafficking of cargo proteins (Fig. 8B).

A 'default pathway' to the vacuole has been mentioned several times. Several groups have reported that Kex2 diverts to the vacuole by default when (i) a portion of its cytosolic, C-terminal tail is deleted (39); (ii) a single tyrosine Tyr_{713} residue in its cytosolic, C-terminal Golgi retention sequence is mutated (41); (iii) *SNX3* is deleted (44) and (iv) as we have shown here, when wild-type α-syn, but not the A30P variant, is expressed (Figs 5 and 6). This default pathway is a vesicular trafficking route from the TGN to the vacuole (32). It should be mentioned that Kex2 localizes to the plasma membrane in yeast cells deficient in the clathrin heavy chain (57). Because we did not observe Kex2-GFP molecules re-localize from punctate Golgi and endosomal structures to the plasma membrane upon the expression of α-syn, we conclude that α-syn does not disrupt the functions of clathrin.

Deleting *SNX3* has a profound effect on Snx3-retromer trafficking of both Ste13 and Kex2. For example, *KEX2-GFP snx3Δ* cells were largely devoid of punctate Golgi and endosomal

structures, and green fluorescence was predominantly found in the vacuole by default (Fig. 5A and B). We expected that under inducing conditions that the *KEX2-GFP snx3Δ* strain carrying the empty vector would have a large and significant reduction in halo size. There was a reduction, but for unknown reasons, it was not significant (Fig. 7A top panel and B). On the other hand, when the same cells were incubated in glucose medium, there was a significant reduction in halo size, which was expected (Fig. 7A bottom panel and C).

Humans have nine orthologs of Kex2, which are expressed in endocrine cells and neurons. The human secretory proprotein convertases (PC) are PC1/3, PC2, furin, PC4, PC5/6, PACE4, PC7, SKI-1/S1P and PCSK9 (58). PCs function to process prohormones, such as proinsulin and proglucagon and neuropeptide precursors, and pro-proteins (both endogenous and viral, including the SARS-CoV-2 spike protein) in various tissues. The level of sequence identity between Kex2, particularly in its catalytic domain and humans PCs is striking. For example, the sequence alignment between Kex2 and the neuroendocrine convertase 1 isoform 2 shows a high-level of sequence similarity ($E = 2e^{-114}$) (Supplementary Material, Fig. S1). The pathways and molecular machinery used for the intracellular trafficking of human PCs are in general poorly defined. One study showed that furin undergoes retrograde trafficking in a Rab9-dependent, retromer-independent manner (59). Whether retrograde trafficking of other PCs is retromer-independent is not known. It will be interesting to study if α-syn affects the trafficking of proprotein convertases in humans.

Neuroendocrine abnormalities, such as disrupted melatonin secretion, insulin resistance, bone metabolism, to name a few, are common in sporadic PD, i.e. such patients have no known mutations in *SNCA* (60). We know of no studies of neuroendocrine abnormalities in PD patients with the A30P or A53T mutations. An obvious question is whether these neuroendocrine abnormalities in the brain come about from α-syn-mediated neuron degeneration of neuropeptide-secreting cells or from the intracellular α-syn aggregation. α-syn is not only expressed in dopaminergic neurons of the mid-brain, but also in the posterior pituitary gland (61), which is a site of hormone secretion, as well as in the cortex (Human protein atlas), which is another area in which neurons secrete neuropeptides (62). The work presented here raises the possibility that α-syn pathology may result in the mistrafficking of PCs in neurons and neuroendocrine cells. Such mistrafficking of the PCs could contribute to the neuroendocrine abnormalities seen in PD patients.

Materials and Methods

Yeast strains, plasmids and antibodies

S. cerevisiae strains and plasmids used in this study are listed in Table 1. Manipulation of yeast strains, preparation of liquid and solid nutrient rich complete medium (YPD) and synthetic complete (SC) or drop out medium were performed following standard protocols (63). Unless stated otherwise, for all experiments, cells transformed with various plasmids were pre-grown in non-inducing selective synthetic medium SC-raffinose lacking nutrients required to maintain the selection of plasmids with auxotrophic markers until mid-log phase. α-Syn expression was induced by replacing raffinose with galactose (2%, wt/vol) (SC-Gal, inducing media). Yeast Snx3-mCherry was expressed under yeast Snx3 promoter cloned in pRS415. The primary antibodies used were mouse anti-α-syn (BD Biosciences, # 610786), rabbit anti-GFP (Abcam; # ab6556), mouse anti-Pgk1 (Abcam, # ab113687) and chicken anti-mCherry (NovusBio, # NBP2–25158). The secondary antibody was goat anti-mouse (Santa Cruz, # SC-516102), goat ant-rabbit (Santa Cruz, # SC-2357) and goat anti-chicken (abcam, # ab97135). Unless otherwise noted, all other chemicals used in this study were purchased from Sigma Aldrich.

Western blotting

Yeast cell lysates were prepared by mechanical glass bead disruption as described previously (55). The lysates were centrifuged (27 000 g/18 min/4°C), and the protein concentrations of the supernatants were determined using DC™ Protein Assay Kit (Bio-Rad 5 000 112). Equal concentration of protein (30 μg) from each sample was boiled for 10 min in 1x Laemmli sample buffer (Bio-Rad catalog # 1610747), resolved by sodium dodecyl sulfate polyacrylamide gel electrophoresis (SDS-PAGE) (4–15% Mini-PROTEAN® TGX™ Precast Protein Gels, Bio-Rad) and transferred onto polyvinylidene fluoride (PVDF) membranes (Trans-Blot® Turbo™ Mini PVDF Transfer Pack, Bio-Rad catalog # 1704156). The membranes were blocked with 5% blotto (G-Biosciences Blot-Quikblocker catalog # 786-011) in phosphate-buffered saline containing 0.1% (v/v) Tween-20 (PBST) for 1 h at room temperature. The membrane was then incubated overnight at 4°C with indicated primary antibodies. Following incubation, immunoreactive bands were detected by incubating with respective horse radish peroxidase (HRP) conjugates. Protein-antibody complexes were visualized using enhanced chemiluminescence substrate (Clarity™ Western ECL Substrate, Bio-Rad #170-5060). The western blot images were acquired using Biorad Chemidoc-MP imaging system and the intensity of Kex2-GFP was quantified and represented as relative protein levels normalized to Pgk1 using ImageJ software.

Fluorescence microscopy

Yeast cells from cultures grown to $OD_{600} \approx 0.5$ were immobilized on agarose pads and three-dimensional image stacks were collected at 0.5-μm z increments spanned across eleven planes along the z-axis using an Olympus AX70 microscope equipped with an Olympus UPlanFl 100×/1.35 NA objective and a CoolSNAP HQ CCD camera (Roper Scientific). Images were acquired at room temperature and were binned (2 × 2). Image acquisition and the z-axis stepping motor (LudI electronic products) were controlled using Slidebook, version 4.0 (Intelligent Imaging Innovations) software. Images were analyzed and quantified using ImageJ software. At least 600 cells were counted per independent clone. The Kex2-GFP puncta-positive cells were quantified after normalizing the low and high value for GFP intensities and eliminating the background intensities and graphically represented.

Halo assay

Cells were grown overnight in roller culture at 24°C in YPD (*MATa bar1*; KT1381) or SC selective medium with raffinose as carbon source (*KEX2-GFP* and *KEX2-GFP snx3Δ*). Synthetic cultures were split and induced by addition of galactose to 2% (wt/vol; SC-Gal, inducing media) for 4 h. 0.5 ml per plate of 1/20 dilution of the KT1381 culture was plated on YPD and YPGal plates and these were allowed to dry 4 h at room temperature. Synthetic cultures were adjusted to 2×10^7 cells/ml (hemacytometer) with SC selective medium with raffinose. For each strain, 1 ml culture was pelleted, and the pellet was resuspended in 5 μl of the same

Table 1. Plasmids and strains

Strain/Plasmid	Genotype/Description	Source
BY4742	*MATα his3Δ1 leu2Δ0 lys2Δ0 ura3Δ0*	Open biosystem
KEX2-GFP	BY4742 *KEX2:GFP::HIS3MX6*	Open biosystem
KEX2-GFP snx3Δ	BY4742 *KEX2:GFP::HIS3MX6 snx3::kanMX4*	This study
KT1381	*MATa leu2 ura3 his3 bar1-1*	Kelly Tatchell
ste13Δ	BY4742 *ste13::kanMX6*	Yeast genome deletion project
ste13Δ snx3Δ	BY4742 *ste13::kanMX6 snx3::HIS3MX6*	This study
pAG426GAL	2 μ, *URA3*, P_{GAL1}	Addgene
pAG425GAL	2 μ, *LEU3*, P_{GAL1}	Addgene
pAG426- α-Syn (WT)	pAG426GAL, P_{GAL1}-α-Syn (WT)	(64)
pAG426-α-Syn (A30P)	pAG426GAL, P_{GAL1}-α-Syn (A30P)	(64)
pAG425-α-Syn (A53T)	pAG425GAL, P_{GAL1}-α-Syn (A53T)	(64)
pAG425-α-Syn(1–100)	pAG425GAL, P_{GAL1}-α-synΔC	This study
pRS415-ySnx3-mCherry	pRS415-Snx3P-ySnx3-Ala10-mCherry	This study

medium. 1 μl per culture was spotted onto each tester lawn in duplicate and plates were incubated at 24°C for 24–30 h before photographing. To minimize error due to variation in size of the alpha factor source (culture) spot as well as deviation of spot shape from a perfect circle, the width of the halo ring around the source was measured rather than the halo diameter. Each ring width was measured at three positions around the halo and the measurements were averaged to generate the width of the band of arrested cells, in millimeters (mm). This value is expressed as halo size. Six halos were measured for each strain/transformant and halo sizes are represented graphically.

Rigor and reproducibility

Ideally, the quantitative assessment of the percentage of cells with green Golgi puncta (Figs 3–6), which involves examining and scoring hundreds of cells, should have been done by a person with no knowledge of the whether the cells express α-syn, A30P or are control EV cells. It was not practical for us to have the analysis done blinded. On the other hand, the true variation in the experiments was captured by using, at minimum, three independent clones (biological replicates) in every experiment; plus, 600 cells were counted per clone. A person (LCR) with no knowledge of the results from the fluorescence experiments carried out the mating assay and analyzed the data independent of the Witt lab. The inclusion of this assay improved the rigor of this study.

Statistical analysis

All data were analyzed using GraphPad Prism (version 6) software. Hypothesis testing method included one-way analysis of variance (ANOVA) with a Bonferroni correction when comparing multiple samples of different treatments to a control. Experimental values are means ± standard deviation of at least three independent experiments and P-value of < 0.05 was considered significant.

Supplementary Material

Supplementary Material is available at *HMG* online

Conflict of Interest statement. The authors declare no competing interests.

Funding

S.N.W. received funding for this work in part from National Institute of Health grant R15 GM131226, the Chancellor of LSUHSC-Shreveport, and the Department of Biochemistry & Molecular Biology, LSUHSC-Shreveport.

References

1. Kalia, L.V. and Lang, A.E. (2015) Parkinson's disease. *Lancet*, **386**, 896–912.
2. Spillantini, M.G., Schmidt, M.L., Lee, V.M., Trojanowski, J.Q., Jakes, R. and Goedert, M. (1997) Alpha-synuclein in Lewy bodies. *Nature*, **388**, 839–840.
3. Goedert, M., Spillantini, M.G., Del Tredici, K. and Braak, H. (2013) 100 years of Lewy pathology. *Nat. Rev. Neurol.*, **9**, 13–24.
4. Polymeropoulos, M.H., Lavedan, C., Leroy, E., Ide, S.E., Dehejia, A., Dutra, A., Pike, B., Root, H., Rubenstein, J., Boyer, R. *et al.* (1997) Mutation in the alpha-synuclein gene identified in families with Parkinson's disease. *Science*, **276**, 2045–2047.
5. Kruger, R., Kuhn, W., Muller, T., Woitalla, D., Graeber, M., Kosel, S., Przuntek, H., Epplen, J.T., Schols, L. and Riess, O. (1998) Ala30Pro mutation in the gene encoding alpha-synuclein in Parkinson's disease. *Nat. Genet.*, **18**, 106–108.
6. Zarranz, J.J., Alegre, J., Gomez-Esteban, J.C., Lezcano, E., Ros, R., Ampuero, I., Vidal, L., Hoenicka, J., Rodriguez, O., Atares, B. *et al.* (2004) The new mutation, E46K, of alpha-synuclein causes Parkinson and Lewy body dementia. *Ann. Neurol.*, **55**, 164–173.
7. Proukakis, C., Dudzik, C.G., Brier, T., MacKay, D.S., Cooper, J.M., Millhauser, G.L., Houlden, H. and Schapira, A.H. (2013) A novel alpha-synuclein missense mutation in Parkinson disease. *Neurology*, **80**, 1062–1064.
8. Lesage, S., Anheim, M., Letournel, F., Bousset, L., Honore, A., Rozas, N., Pieri, L., Madiona, K., Duerr, A., Melki, R. *et al.* (2013) G51D alpha-Synuclein mutation causes a novel parkinsonian-pyramidal syndrome. *Ann. Neurol.*, **73**, 459–471.
9. Singleton, A.B., Farrer, M., Johnson, J., Singleton, A., Hague, S., Kachergus, J., Hulihan, M., Peuralinna, T., Dutra, A., Nussbaum, R. *et al.* (2003) Alpha-synuclein locus triplication causes Parkinson's disease. *Science*, **302**, 841–841.
10. Conway, K.A., Harper, J.D. and Lansbury, P.T. (1998) Accelerated in vitro fibril formation by a mutant alpha-synuclein linked to early-onset Parkinson disease. *Nat. Med.*, **4**, 1318–1320.
11. Willingham, S., Outeiro, T.F., DeVit, M.J., Lindquist, S.L. and Muchowski, P.J. (2003) Yeast genes that enhance the toxicity

of a mutant Huntingtin fragment or alpha-synuclein. *Science*, **302**, 1769–1772.
12. Ben Gedalya, T., Loeb, V., Israeli, E., Altschuler, Y., Selkoe, D.J. and Sharon, R. (2009) Alpha-Synuclein and polyunsaturated fatty acids promote clathrin-mediated endocytosis and synaptic vesicle recycling. *Traffic*, **10**, 218–234.
13. Burre, J., Sharma, M., Tsetsenis, T., Buchman, V., Etherton, M.R. and Sudhof, T.C. (2010) Alpha-Synuclein promotes SNARE-complex assembly in vivo and in vitro. *Science*, **329**, 1663–1667.
14. Logan, T., Bendor, J., Toupin, C., Thorn, K. and Edwards, R.H. (2017) Alpha-Synuclein promotes dilation of the exocytotic fusion pore. *Nat. Neurosci.*, **20**, 681–689.
15. Weinreb, P.H., Zhen, W., Poon, A.W., Conway, K.A. and Lansbury, P.T.J. (1996) NACP, a protein implicated in Alzheimer's disease and learning, is natively unfolded. *Biochemistry*, **35**, 13709–13715.
16. Chandra, S., Chen, X.C., Rizo, J., Jahn, R. and Sudhof, T.C. (2003) A broken alpha-helix in folded alpha-synuclein. *J. Biol. Chem.*, **278**, 15313–15318.
17. Bartels, T., Choi, J.G. and Selkoe, D.J. (2011) Alpha-Synuclein occurs physiologically as a helically folded tetramer that resists aggregation. *Nature*, **477**, 107–110.
18. Lashuel, H.A., Petre, B.M., Wall, J., Simon, M., Nowak, R.J., Walz, T. and Lansbury, P.T. (2002) Alpha-Synuclein, especially the Parkinson's disease-associated mutants, forms pore-like annular and tubular protofibrils. *J. Mol. Biol.*, **23**, 1089–1102.
19. Hashimoto, M., Hsu, L.J., Sisk, A., Xia, Y., Takeda, A., Sundsmo, M. and Masliah, E. (1998) Human recombinant NACP/alpha-synuclein is aggregated and fibrillated in vitro: relevance for Lewy body disease. *Brain Res.*, **799**, 301–306.
20. Volles, M.J., Lee, S.J., Rochet, J.C., Shtilerman, M.D., Ding, T.T., Kessler, J.C. and Lansbury, P.T.J. (2001) Vesicle permeabilization by protofibrillar alpha-synuclein: implications for the pathogenesis and treatment of Parkinson's disease. *Biochemistry*, **40**, 7812–7819.
21. Kayed, R., Sokolov, Y., Edmonds, B., McIntire, T.M., Milton, S.C., Hall, J.E. and Glabe, C.G. (2004) Permeabilization of lipid bilayers is a common conformation-dependent activity of soluble amyloid oligomers in protein misfolding diseases. *J. Biol. Chem.*, **279**, 46363–46366.
22. Vilarino-Guell, C., Wider, C., Ross, O.A., Dachsel, J.C., Kachergus, J.M., Lincoln, S.J., Soto-Ortolaza, A.I., Cobb, S.A., Wilhoite, G.J., Bacon, J.A. *et al.* (2011) VPS35 mutations in Parkinson disease. *Am. J. Hum. Genet.*, **89**, 162–167.
23. Zimprich, A., Benet-Pages, A., Struhal, W., Graf, E., Eck, S.H., Offman, M.N., Haubenberger, D., Spielberger, S., Schulte, E.C., Lichtner, P. *et al.* (2011) A mutation in VPS35, encoding a subunit of the retromer complex, causes late-onset Parkinson disease. *Am. J. Hum. Genet.*, **89**, 168–175.
24. Lesage, S., Condroyer, C., Klebe, S., Honore, A., Tison, F., Brefel-Courbon, C., Durr, A., Brice, A. and French Parkinsons Dis Genetics, S. (2012) Identification of VPS35 mutations replicated in french families with parkinson disease. *Neurology*, **78**, 1449–1450.
25. Seaman, M.N. (2005) Recycle your receptors with retromer. *Trends Cell Biol.*, **15**, 68–75.
26. Small, S.A. and Petsko, G.A. (2015) Retromer in Alzheimer disease, Parkinson disease and other neurological disorders. *Nat. Rev. Neurosci.*, **16**, 126–132.
27. Williams, E.T., Chen, X. and Moore, D.J. (2017) VPS35, the retromer complex and Parkinson's disease. *J. Parkinsons Dis.*, **7**, 219–233.
28. Haft, C.R., Sierra, M.D.L., Bafford, R., Lesniak, M.A., Barr, V.A. and Taylor, S.I. (2000) Human orthologs of yeast vacuolar protein sorting proteins Vps 26, 29, and 35: assembly into multimeric complexes. *Mol. Biol. Cell*, **11**, 4105–4116.
29. Seet, L.F. and Hong, W.J. (2006) The Phox (PX) domain proteins and membrane traffic. *Biochim. Biophys. Acta*, **1761**, 878–896.
30. Carlton, J., Bujny, M., Peter, B.J., Oorschot, V.M.J., Rutherford, A., Mellor, H., Klumperman, J., McMahon, H.T. and Cullen, P.J. (2004) Sorting nexin-1 mediates tubular endosome-to-TGN transport through coincidence sensing of high-curvature membranes and 3-phosphoinositides. *Curr. Biol.*, **14**, 1791–1800.
31. Cullen, P.J. and Korswagen, H.C. (2012) Sorting nexins provide diversity for retromer-dependent trafficking events. *Nat. Cell Biol.*, **14**, 29–37.
32. Roberts, C.J., Nothwehr, S.F. and Stevens, T.H. (1992) Membrane protein sorting in the yeast secretory pathway: evidence that the vacuole may be the default compartment. *J. Cell Biol.*, **119**, 69–83.
33. Askwith, C., Eide, D., Vanho, A., Bernard, P.S., Li, L.T., Davis-kaplan, S., Sipe, D.M. and Kaplan, J. (1994) The FET3 gene of *Saccharomyces-cerevisiae* encodes a multicopper oxidase required for ferrous iron uptake. *Cell*, **76**, 403–410.
34. Dancis, A., Yuan, D.S., Haile, D., Askwith, C., Eide, D., Moehle, C., Kaplan, J. and Klausner, R.D. (1994) Molecular characterization of a copper transport protein in *Saccharomyces-cerevisiae* - an unexpected role for copper in iron transport. *Cell*, **76**, 393–402.
35. Stearman, R., Yuan, D.S., Yamaguchi Iwai, Y., Klausner, R.D. and Dancis, A. (1996) A permease-oxidase complex involved in high-affinity iron uptake in yeast. *Science*, **271**, 1552–1557.
36. Strochlic, T.I., Setty, T.G., Sitaram, A. and Burd, C.G. (2007) Grd19/Snx3p functions as a cargo-specic adapter for retromer-dependent endocytic recycling. *J. Cell Biol.*, **177**, 115–125.
37. Strochlic, T.I., Schmiedekamp, B.C., Lee, J., Katzmann, D.J. and Burd, C.G. (2008) Opposing activities of the snx3-retromer complex and escrt proteins mediate regulated cargo sorting at a common endosome. *Mol. Biol. Cell*, **19**, 4694–4706.
38. Rockwell, N.C. and Thorner, J.W. (2004) The kindest cuts of all: crystal structures of Kex2 and furin reveal secrets of precursor processing. *Trends Biochem. Sci.*, **29**, 80–87.
39. Fuller, R.S., Brake, A.J. and Thorner, J. (1989) Intracellular targeting and structural conservation of a prohormone-processing endoprotease. *Science*, **246**, 482–486.
40. Nothwehr, S.F., Roberts, C.J. and Stevens, T.H. (1993) Membrane-protein retention in the yeast golgi-apparatus - dipeptidyl aminopeptidase-a is retained by a cytoplasmic signal containing aromatic residues. *J. Cell Biol.*, **121**, 1197–1209.
41. Wilcox, C.A., Redding, K. and Fuller, R.S. (1992) Mutation of a tyrosine localization signal in the cytosolic tail of yeast Kex2 protease disrupts Golgi retention and result sin default transport to the vacuole. *Mol. Biol. Cell*, **3**, 1353–1371.
42. Brickner, J.H. and Fuller, R.S. (1997) SOI1 encodes a novel, conserved protein that promotes TGN-endosomal cycling of Kex2p and other membrane proteins by modulating the function of two TGN localization signals. *J. Cell Biol.*, **139**, 23–36.
43. Harrison, M.S., Hung, C.S., Liu, T.T., Christiano, R., Walther, T.C. and Burd, C.G. (2014) A mechanism for retromer endosomal coat complex assembly with cargo. *Proc. Natl. Acad. Sci. U. S. A.*, **111**, 267–272.

44. Voos, W. and Stevens, T.H. (1998) Retrieval of resident late-Golgi membrane proteins from the prevacuolar compartment of *Saccharomyces cerevisiae* is dependent on the function of Grd19p. *J. Cell Biol.*, **140**, 577–590.
45. Patel, D., Xu, C., Nagarajan, S., Liu, Z.C., Hemphill, W.O., Shi, R.H., Uversky, V.N., Caldwell, G.A., Caldwell, K.A. and Witt, S.N. (2018) Alpha-synuclein inhibits Snx3-retromer-mediated retrograde recycling of iron transporters in S. cerevisiae and C. elegans models of Parkinson's disease. *Hum. Mol. Genet.*, **27**, 1514–1532.
46. Nothwehr, S.F., Bryant, N.J. and Stevens, T.H. (1996) The newly identified yeast GRD genes are required for retention of late-Golgi membrane proteins. *Mol. Cell. Biol.*, **16**, 2700–2707.
47. Julius, D., Blair, L., Brake, A., Sprague, G. and Thorner, J. (1983) Yeast alpha factor is processed froma larger precursor polypeptide: the essential role of a membrane-bound dipeptidyl aminopeptidase. *Cell*, **32**, 839–852.
48. Zhou, A., Webb, G., Zhu, X.R. and Steiner, D.F. (1999) Proteolytic processing in the secretory pathway. *J. Biol. Chem.*, **274**, 20745–20748.
49. Redding, K., Holcomb, C. and Fuller, R.S. (1991) Immunolocalization of Kex2 protease identifies putative late Golgi compartment in the yeast Saccharomyces cerevisiae. *J. Cell Biol.*, **113**, 527–538.
50. Pasanen, P., Myllykangas, L., Siitonen, M., Raunio, A., Kaakkola, S., Lyytinen, J., Tienari, P.J., Poyhonen, M. and Paetau, A. (2014) A novel alpha-synuclein mutation A53E associated with atypical multiple system atrophy and Parkinson's disease-type pathology. *Neurobiol. Aging*, **35**, 2180, e1-5.
51. Yoshino, H., Hirano, M., Stoessl, A.J., Imamichi, Y., Ikeda, A., Li, Y.Z., Funayama, M., Yamada, I., Nakamura, Y., Sossi, V. *et al.* (2017) Homozygous alpha-synuclein p.A53V in familial Parkinson's disease. *Neurobiol. Aging*, **57**(248), e7, e12–e248.
52. Wang, W., Nguyen, L.T.T., Burlak, C., Chegini, F., Guo, F., Chataway, T., Ju, S.L., Fisher, O.S., Miller, D.W., Datta, D. *et al.* (2016) Caspase-1 causes truncation and aggregation of the Parkinson's disease-associated protein alpha-synuclein. *Proc. Natl. Acad. Sci. U. S. A.*, **113**, 9587–9592.
53. Sorrentino, Z.A., Vijayaraghavan, N., Gorion, K.M., Riffe, C.J., Strang, K.H., Caldwell, J. and Giasson, B.I. (2018) Physiological C-terminal truncation of alpha-synuclein potentiates the prion-like formation of pathological inclusions. *J. Biol. Chem.*, **293**, 18914–18932.
54. Outeiro, T.F. and Lindquist, S. (2003) Yeast cells provide insight into alpha-synuclein biology and pathobiology. *Science*, **302**, 1772–1775.
55. Flower, T.R., Chesnokova, L.S., Froelich, C.A., Dixon, C. and Witt, S.N. (2005) Heat shock prevents alpha-synuclein-induced apoptosis in a yeast model of Parkinson's disease. *J. Mol. Biol.*, **351**, 1081–1100.
56. Manney, T.R. (1983) Expression of the Bar1 gene in Saccharomyces cerevisiae: induction by the alpha mating pheromone of an activity associated with secreted protein. *J. Bacteriol.*, **155**, 291–301.
57. Payne, G.S. and Schekman, R. (1989) Clathrin: a role in the intracellular retention of a Golgi membrane protein. *Science*, **245**, 1358–1365.
58. Seidah, N.G., Sadr, M.S., Chretien, M. and Mbikay, M. (2013) The multifaceted proprotein convertases: their unique, redundant, complementary, and opposite functions. *J. Biol. Chem.*, **288**, 21473–21481.
59. Chia, P.Z.C., Gasnereau, I., Lieu, Z.Z. and Gleeson, P.A. (2011) Rab9-dependent retrograde transport and endosomal sorting of the endopeptidase furin. *J. Cell Sci.*, **124**, 2401–2413.
60. De Pablo-Fernandez, E., Breen, D.P., Bouloux, P.M., Barker, R.A., Foltynie, T. and Warner, T.T. (2017) Neuroendocrine abnormalities in Parkinson's disease. *J. Neurol. Neurosurg. Psychiatry*, **88**, 176–185.
61. Homma, T., Mochizuki, Y. and Mizutani, T. (2012) Phosphorylated a-synuclein immunoreactivity in the posterior pituitary lobe. *Neuropathology*, **32**, 385–389.
62. Smith, S.J., Sumbul, U., Graybuck, L.T., Collman, F., Seshamani, S., Gala, R., Gliko, O., Elabbady, L., Miller, J.A., Bakken, T.E. *et al.* (2019) Single-cell transcriptomic evidence for dense intracortical neuropeptide networks. *elife*, **8**, e47889.
63. Burke, D., Dawson, D. and Stearns, T. (2000) *Methods in Yeast Genetics. Cold Spring Harbor Lab Press*. Cold Spring Harbor, NY.
64. Lee, Y.J., Wang, S., Slone, S.R., Yacoubian, T.A. and Witt, S.N. (2011) Defects in very long chain fatty acid synthesis enhance alpha-synuclein toxicity in a yeast model of Parkinson's disease. *PLoS One*, **6**, e15946.
65. Wilcox, C.A. and Fuller, R.S. (1991) Posttranslational processing of the prohormone-cleaving Kex2 protease in the Saccharomyces cerevisiae secretory pathway. *J. Cell Biol.*, **115**, 297–307.